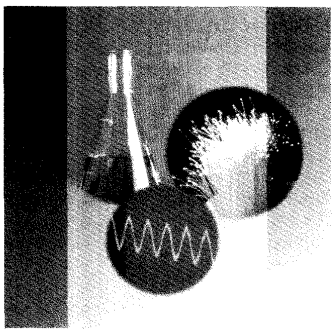

Optical Oximetry Sensors for Whole Blood and Tissue

Setsuo Takatani
Jian Ling
Department of Surgery
Baylor College of Medicine

The oxygen saturation of hemochromes such as hemoglobin, myoglobin, and cytochromes yield useful information for evaluation of patients in various clinical settings. In particular, clinical measurements of hemoglobin saturation in major vessels and cardiac chambers have been reported during catheterization for detection of cardiac shunts [1-2], for estimation of cardiac output from arterio-venous oxygen difference via Fick's principle [3], and for monitoring patients with various cardiac diseases [4-6]. During surgical procedures and recovery from anesthesia, hemoglobin oxygen saturation has been utilized for early detection of hypoxia [7-8]. And in the care of fetuses and neonates, oxygen saturation data are useful [9-12].

The measurement of oxygen saturation in humans goes back to the 1940s, when Millikan devised an instrument to measure arterial saturation from the forehead [13]. This was followed by various workers including Brinkman, Wood, Sekelj, Tait, et al., who noninvasively estimated arterial saturation as well as tissue oxygen saturation [14-17]. The works by Wood and co-workers resulted in ear oximeters, and the contributions by Sekelj, et al. advanced this device. In the 1960s, solid state devices such as the light emitting diode and photodiode were introduced to make a miniature skin reflectance sensors and also intravascular measurement systems by utilizing fiber optic guides. The fiber optic intravascular oximeter developed by Polanyi and Hehir [18] became the basis for the modern invasive oximeter.

In the 1970s, Cheung and Reynolds [19-20] modeled the optical fiber system in blood, based on the photon diffusion theory developed by Johnson [21]. Noninvasive skin and tissue reflectance oximeters were also developed by Cohen and Takatani [22-23] in the late 1970s, with optical propagation in the medium modeled utilizing one-dimensional and three-dimensional photon diffusion theory. Contrary to the transport theory approach, Lubbers, et al. [24-25] utilized the multi-component approach in combination with Monte-Carlo simulation in analyzing the tissue spectra. However, problems of the earlier workers included 1) lack of adequate calibration procedure in vivo, 2) unknown distribution of arterial-to-venous blood volume in tissue, 3) unknown optical path-length in tissue, and 4) lack of an appropriate mathematical relation to calculate tissue hemoglobin saturation in vivo.

In the early 1980s, the innovative approach of pulse oximetry, which combined the principle of conventional optical oximetry with the plethysmographic principle, offered a means of noninvasively estimating arterial blood oxygen saturation [26-30]. This instrument assumes that the forward scattered plethymographic pulsatile signals are due to arterial blood, and noninvasively measures arterial saturation from the finger tip or the ear lobe. Most operating rooms and intensive care units today are equipped with this device. Another innovative approach is the use of a very narrow light pulse (on the order of picoseconds) or ultra high frequency signal (on the order of 500 MHz) to measure transit time of light signals through tissues. These techniques characterize the tissue optical properties of absorption and scattering, from which absolute tissue oxygen saturation can be estimated [31-34]. Although this approach is still in the experimental state, it offers an absolute determination of tissue oxygen saturation as well as an image of the tissue oxygen field in a three dimensions [35-36].

This article reviews the optical techniques applied to the determination of intravascular hemoglobin oxygen saturation as well as the noninvasive estimation of arterial and tissue saturation. Although in skeletal muscles and brain tissues myoglobin and cytochrome analyses have been demonstrated [37-38], their effects upon absorption and reflection spectra of tissues are small. Thus, this review is focused only upon measurement of hemoglobin saturation.

Basis of Optical Oximetry

Optical oximetry can be classified into a) transmission or forward scattering and b) reflection or back scattering type (Fig. 1). In forward scattering, a target area is illuminated with a light source, and transmitted or forward scattered light is analyzed. In the reflection mode,

 0739-5175/94/$4.00©1994

Authorized licensed use limited to: Kansas State University. Downloaded on October 09,2021 at 04:47:57 UTC from IEEE Xplore. Restrictions apply.

APL_MAS_ITC_00374038
RX-0498.0001
APPLE 1085
Apple v. Masimo
IPR2024-00243

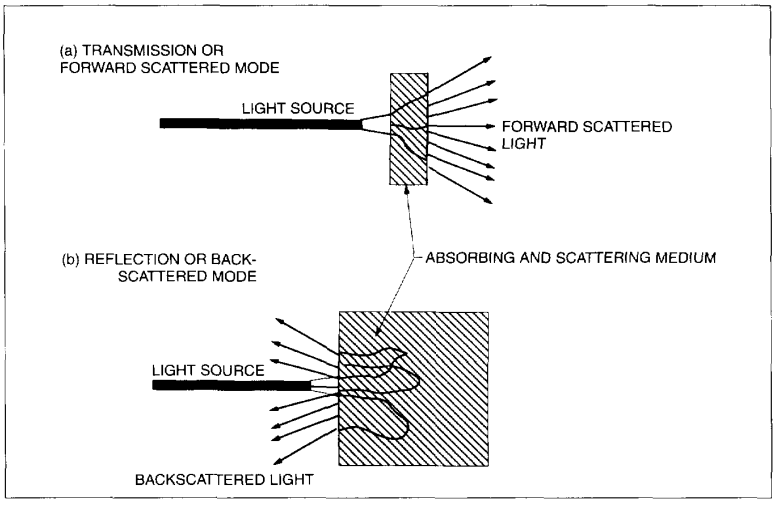

1. Principle of (a) transmission or forward scattered, and (b) reflection or backward scattered optical spectroscopy.

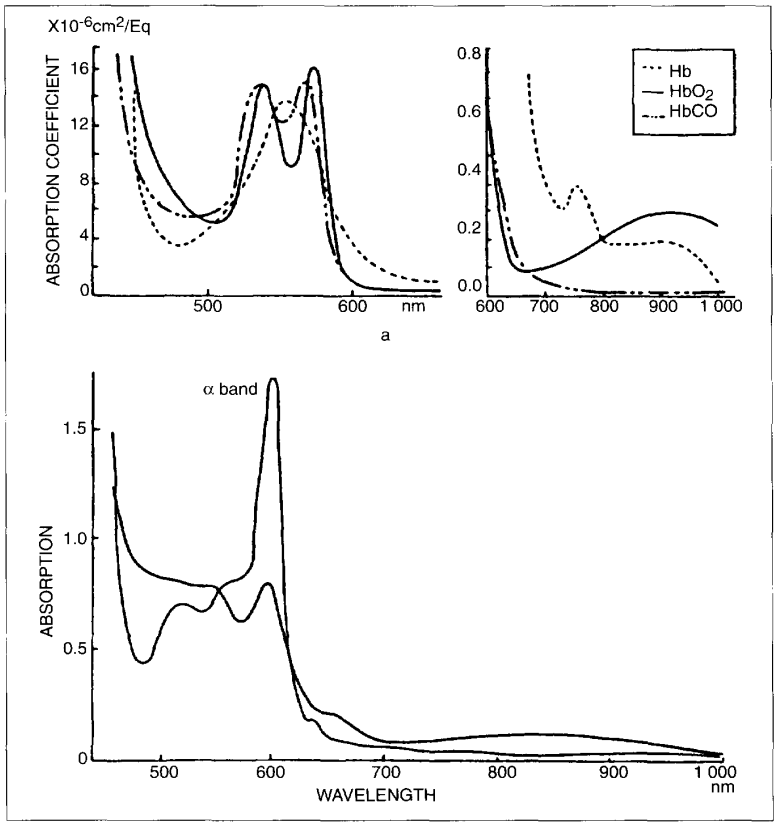

2. Absorption spectra of hemoglobin, myoglobin, bilirubin and cytochrome aa3 in visible and near-infrared wavelength.

backscattered light from the specimen is sampled to estimate the oxygen saturation. In both methods, absorption (K) and scattering (S) properties of the tissue sample plays a major role. In particular, wavelength dependent absorption properties of various species such as hemoglobin, myoglobin, cytochrome aa3 contained in the tissue sample will affect the measured transmittance and reflectance.

Figure 2 shows the absorption spectra of these hemochromes in the visible and near-infrared regions [39-40]. In normal tissue, when the transmission and reflection spectra are examined, they strongly depend on the absorption spectra of hemoglobin, since the concentration is much greater than other species.

Absorption Constant

In relation to blood and tissue oximetry, absorption of light by hemoglobin in the wavelength ranges between 450 and 550 nm is significantly larger (about 10 times) in comparison to the wavelength range between 650-1000 nm (Fig. 2). Bench top oximeters usually sample absorption spectra at around 550 nm, while intravascular and tissue oximetry utilize the wavelength range of 650-1000 nm. The wavelength of 805 nm is called isosbestic, where there is no absorption difference between the oxy- and deoxy-hemoglobin.

As the hemoglobin is contained inside the red blood cells (RBC), a microscopic absorption cross section of RBCs, σ in μ^2, is usually used to describe absorption properties, either as oxygenated cross section, so or deoxygenated, σ_r. Microscopic absorption cross section of RBCs can be derived from the specific absorption coefficients of hemoglobin using the known absorption cross section at a specific wavelength. The macroscopic absorption constant of blood, K_b in mm^{-1} is obtained by multiplying the microscopic cross section, σ, by concentration of RBCs (hematocrit, $H/\overline{V}$), i.e., $K_b = H\sigma/\overline{V}$. For a given oxygen saturation SO_2 of whole blood, K_b is expressed as a linear sum of σ_o and σ_r as follows:

$$K_b = H\frac{\sigma}{\overline{V}} = \frac{H}{\overline{V}}(\sigma_o\, SO_2 + \sigma_r\,(1-SO_2)) \qquad (1)$$

A compound system of tissue can be treated as a homogeneous mixture of blood and blood-less tissue, and blood volume fraction, V_b, can be used to obtain the net absorption constant of tissue, K_T, as follows:

$$K_T = K_t\,(1-V_b) + K_b V_b \qquad (2)$$

where, K_t is the macroscopic absorption constant of the blood-less tissue. Typical K_t values of various tissues range from 0.03 to 10.0 mm^{-1} [37, 41-46]. Further,

Authorized licensed use limited to: Kansas State University. Downloaded on October 09,2021 at 04:47:57 UTC from IEEE Xplore. Restrictions apply.

APL_MAS_ITC_00374039
RX-0498.0002

blood in tissue can be treated as a sum of arterial and venous blood, and V_b can be given as:

$$V_b = V_a + V_v \tag{3}$$

where V_a and V_v are the arterial and venous fractional blood volume in tissue, respectively. Equation 1 can be divided into a component for arterial saturation, S_aO_2, and the one for venous saturation S_vO_2 as follows:

$$K_{ba} = \frac{H}{\bar{V}}(\sigma_o S_a O_2 + \sigma_r(1-S_a O_2)) \tag{4}$$

$$K_{bv} = \frac{H}{\bar{V}}(\sigma_o S_v O_2 + \sigma_r(1-S_v O_2)) \tag{5}$$

where K_{ba} and K_{bv} are the macroscopic absorption constants of arterial and venous blood, respectively. Then, The net absorption constant due to mixture of the arterial and venous blood, K_b' becomes:

$$K_b' = K_{ba}V_{ba} + K_{bv}V_{bv} \tag{6}$$

Thus, the net absorption constant of the tissue becomes

$$K_T = K_t\,[1-(V_a+V_v)] + K_b' \tag{7}$$

The net tissue oxygen saturation, SO_{2T}, averaged over the arterial and venous blood, can be expressed as:

$$SO_{2T} = S_a O_2 V_a + S_v O_2 V_v \tag{8}$$

This is the oxygen saturation of tissue when transmitted or reflected light from tissue is analyzed. When we discuss tissue oxygenation utilizing time resolved spectroscopy, SO_{2T} is the target measurement from which venous saturation and arterial to venous blood volume distribution can be derived.

Scattering Constant

Scattering of light by red blood cells and tissue components takes place at interfaces where there is a change in the index of refraction. This scattering is due to microscopic fluctuations in the refractive index of the tissue, corresponding to physical inhomogeneities. The angles through which the light is scattered and the scatter coefficient depend on the size and shape of the optical inhomogeneities relative to the wavelength, and to differences in the refractive index between the inhomogeneities and the surrounding medium. Scattering from molecules or structures whose size is much less than the wavelength (Rayleigh scattering), is weak, nearly equal in all directions (isotropic scattering), and rapidly decreases with wavelength. When the wavelength and inhomogeneities are about the same size, the scattering is stronger, is more forward-directed, and decreases roughly inversely with the wavelength. Scattering from large inhomogeneities is highly forward-directed and only weakly dependent on wavelength (Mie scattering).

The RBC is biconcave in shape, with outer diameter of about 8 μm and average thickness of about 1 μm. The average volume of a human RBC is about 87 μm^3. Again, the microscopic scattering cross section of a RBC is defined as σ_s, where this value denotes total scattering cross section and comprises forward scattering cross sections σ_s^+, and backscattering cross section σ_s^-. The index of anisotropicity is defined as: $w = (\sigma_s^+ - \sigma_s^-)/(\sigma_s^+ + \sigma_s^-)$. When the particle is totally forward scattering, w = 1, while totally backscattering, w= -1. The w of RBC ranges from 0.7 to 0.967, and is strongly forward scattering. The scattering characteristics of RBC and tissue components are wavelength dependent. The backscattering cross section of RBC in the visible and near-infrared regions is approximately constant. In the near-infrared region above 800 nm, since the absorption by the hemoglobin is smaller, the light particle can propagate deeper into tissue. Scattering cross sections of the RBCs have been described theoretically using a sphere model by Mie theory [19,20,47], a disk model by the Rayleigh-Gans method [19,20], and a more complicated discoid model by a WKB method [48]. These values have been compared against experimental values and used to explain experimental results.

Again, the macroscopic scattering constant of the blood can be given by:

$$S_b = \frac{H}{\bar{V}}\sigma_s \tag{9}$$

where σ_s is the total scattering cross section given by $\sigma = \sigma_s^+ + \sigma_s^-$. However, in a single phase material there will be no scattering, i.e., when RBCs are packed (H = 100%) or when there are no RBCs (H = 0). Thus, Eq. 8 is usually multiplied by (1 - H) [49], giving:

$$S'_b = S_b(1-H) = \frac{H}{\bar{V}}(1-H)\sigma \tag{10}$$

For a compound system such as tissue, the linear treatment used in the absorption analysis is also applicable. Thus, the net scattering constant of tissue, S_T, is expressed as:

$$S_T = S_t(1-V_b) + S_b'V_b \tag{11}$$

Here, S_t is the scattering constant of the bloodless tissue component. Usually, since the absorption constant of arterial and venous blood do not deviate significantly, that is oxygen saturation does not affect scattering properties of RBCs, Eq. 11 can be used to express the macroscopic scattering constant of compound tissue.

Theoretical Analysis of Optical Propagation in Tissue

Theoretical analysis of optical propagation can be divided into 1) absorbing but no scattering, and 2) both absorbing and scattering.

Absorbing but Non-Scattering Medium

In the case of non-scattering but absorbing medium, the simple Beer-Lambert Law can be applied to analyze the transmitted light intensity in terms of various species concentrations. Here, the transmitted intensity of light, I_t, is related to the incident light intensity, I_o, by:

$$I_t = I_o e^{-\alpha Ct} \tag{12}$$

$$OD = \ln(I_o/I_t) = \alpha Ct \tag{13}$$

where α is the absorption coefficient, C the concentration of the absorber, and t is the optical pathlength. This equation can be applied to a homogeneous and non-scattering solution. In Eq. 13, OD is the optical density, a linear function of concentration, C, when optical pathlength, t, is fixed. Bench top oximeters usually utilize from 2 to 4 wavelengths, depending on the number of components involved in the system. Equation 13 is utilized to solve for the concentration of the species, from which saturation can be derived. For example, when two wavelengths are used, from Eq. 13, concentrations of oxy- and deoxy-hemoglobin, C_{HbO2} and C_{Hb}, are given as:

$$C_{Hb} = \frac{n}{d}$$

where

$n = OD(\lambda_1)\alpha(\lambda_2 Hb) - OD(\lambda_2)\alpha(\lambda_1 Hb)$

and

$d = t\,[\alpha(\lambda_1 HbO2)\alpha(\lambda_2 Hb) - \alpha(\lambda_2 HBO2)\alpha(\lambda_1 Hb)]$ (14)

$$C_{Hb} = \frac{n}{d}$$

where

$n = OD\,(\lambda_1)\alpha(\lambda_2 HbO2) - OD(\lambda_2)\,\alpha(\lambda_1 HbO2)$

and

$d = t\,[\alpha(\lambda_1 Hb)\,\alpha(\lambda_2 HbO2) - \alpha(\lambda_2 Hb)\,\alpha(\lambda_1 HbO2)]$ (15)

Authorized licensed use limited to: Kansas State University. Downloaded on October 09,2021 at 04:47:57 UTC from IEEE Xplore. Restrictions apply.

APL_MAS_ITC_00374040
RX-0498.0003

In Eqs. 14 and 15, $\alpha(\lambda_1 Hb)$ and $\alpha(\lambda_1 HbO2)$ are the absorption coefficients of Hb and HbO2, respectively, at wavelength λ_1, and $\alpha(\lambda_2 Hb)$ and $\alpha(\lambda_2 HbO2)$ are the absorption coefficients of Hb and HbO2, respectively, at wavelength λ_2. Then, from Eqs. 14 and 15, the oxygen saturation can be derived as:

$$SO_2 = \frac{C_{HbO2}}{C_{HbO2} + C_{Hb}}$$

Absorbing and Scattering Medium

When the medium is both scattering and absorbing, the non-liner effect of scattering becomes important and the result deviates from Eq. 13. The first theoretical treatment of scattering in a random medium was given in 1903 by Schuster [50], who described interactions of radiation with the foggy atmosphere. This one-dimensional theory was based on phenomenological observations of intensity transfer in the medium. It was further heuristically developed in 1931 by Kubelk and Munk [51], by which time it was called the "two-flux theory." Based on the concept of forward and backward traveling fluxes, it adequately describes optical propagation in a medium if the illumination is diffuse and the medium is dull so that light is diffusely scattered (Fig. 3). However, because of its phenomenological and heuristic nature, as well as its one-dimensionality, the theory has serious limitations when applied to optical processes in whole blood and tissue.

The optical process can be classified into a) single scattering, b) multiple scattering and 3) diffusion, depending on the concentration of scatterers as shown in Fig. 4. Various scattering theories are available for a single particle, including Mie theory, which deals with scattering of light by a sphere; and Rayleigh-Gans theory for scattering by a disk. When the particle concentration increases, a phenomenon called "multiple scattering" occurs. The light goes through multiple scatterings because of the existence of numerous particles in the medium. In application to biological samples, such as whole blood and tissue, Twersky developed a forward scattering theorem [49]. It includes both absorption and scattering terms in a modification of Eq. 12, and as given by:

$$I_t = I_0 e^{-ST} + q(1-e^{-ST})e^{-\alpha Ct} \qquad (16)$$

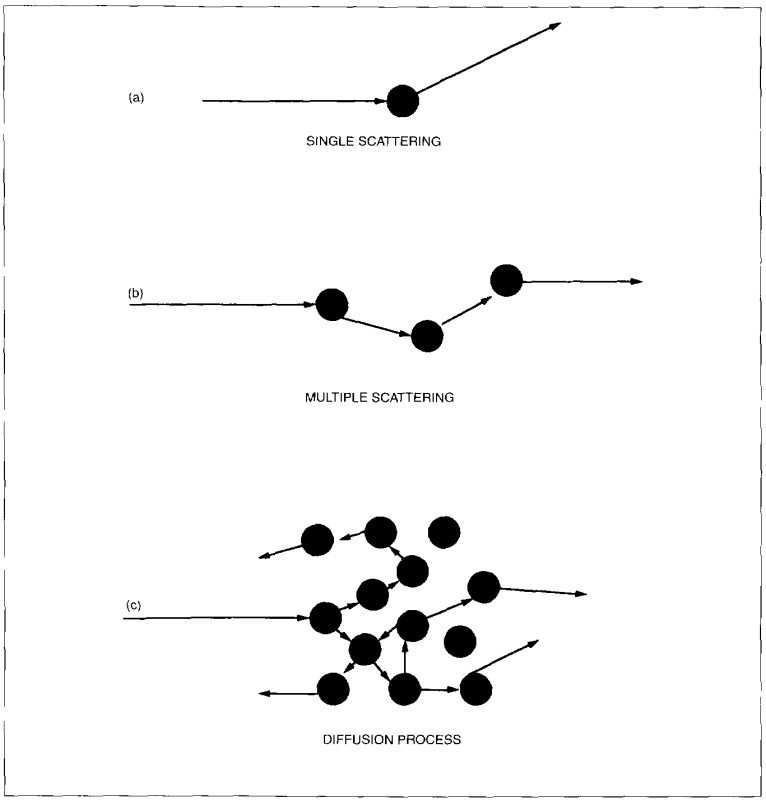

3. Schematic drawing of (a) single scattering, (b) multiple scattering, and (c) diffusion processes.

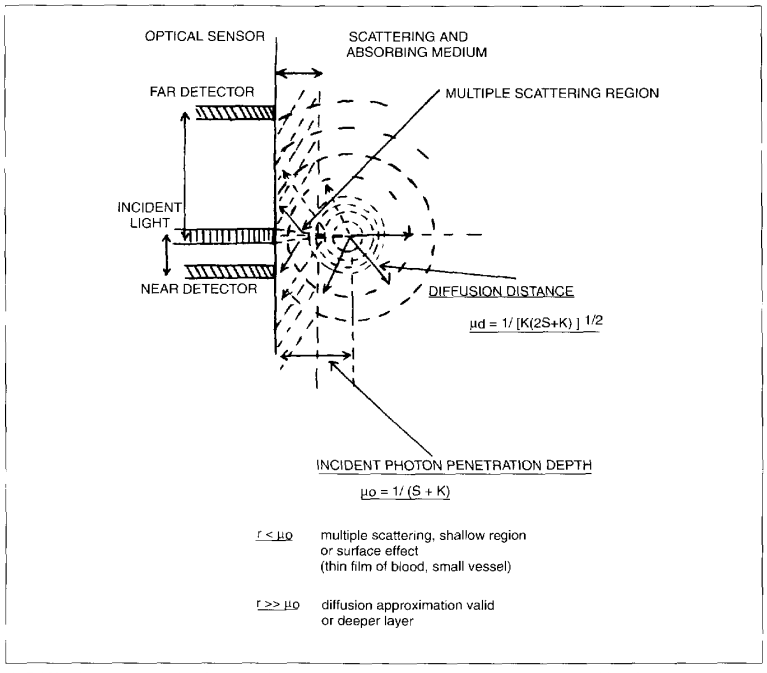

4. Diffusion process in the medium, and underlying assumptions for diffusion process.

Authorized licensed use limited to: Kansas State University. Downloaded on October 09,2021 at 04:47:57 UTC from IEEE Xplore. Restrictions apply.

APL_MAS_ITC_00374041
RX-0498.0004

Then, OD becomes:

$$OD = B + \alpha Ct \quad (17)$$

Here, B is the term related to scattering and the second term is related to absorption. For the multiple scattering analysis to be applicable, the medium thickness must be very thin or the concentration of the particles must be very low, so that the coherence of the incoming light is not lost. Equation 16 has been successfully applied to analysis of light transmitted through a small vessel, through a frozen tissue sample, and in the vicinity of the optical fiber tips.

When the particle concentration increases above 5%, or the medium thickness becomes large so that light will go through repeated multiple scattering, then the coherence of the incident light is lost and it is said the light becomes diffused [52]. This was confirmed in whole blood with an immersed optical fiber. As the hematocrit of blood increased, the light patterns became more and more centered around the tip of optical fiber, and coherence of the incident light was completely lost [21].

Thus, as shown in Fig. 5, diffusion takes place, when the medium satisfies the conditions of a) scattering particle concentration above the critical value, and b) the medium thickness becomes large. We can define two parameters to evaluate the underling assumptions of diffusion theory. First, incident photon penetration depth, δ_o, and defined as 1/(S + K), will indicate the average depth, t_D in which the light can penetrate into a particular medium before losing coherence. Thus, it is entirely function of the medium and excitation wavelength, λ. The second parameter is the diffusely scattering condition, called albedo, and defined as S/(S + K). The albedo, as S and K are also wavelength dependent, is determined by the medium and the excitation wavelength . When the albedo of the medium is greater than 0.5, diffusion will take place. When the medium satisfies both conditions, diffusion analysis is valid. Diffusion analysis is a heuristic approach derived from transport theory. Its application to biological media such as whole blood and tissues has been employed by several researchers. The diffusion approach can be divided into two phases: a) steady state continuous case, and b) a time resolved or pulse diffusion case.

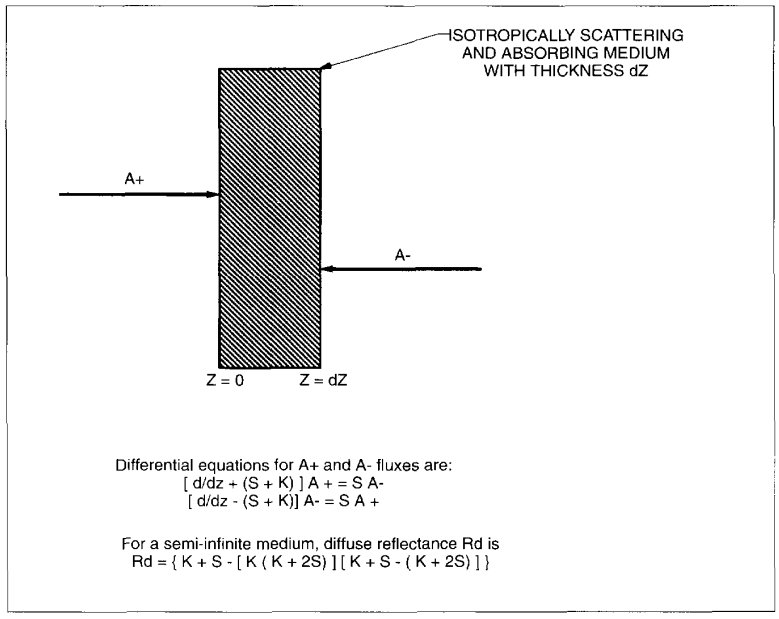

5. Two flux analysis

Diffusion analysis

a. Steady state diffusion equation

For the steady state case, the diffusion equation was derived from the transport theory and given in the cylindrical coordinate by [21]:

$$(\Delta^2 - f_a / D)\, \rho_s(r,\theta,z) = So(r,\theta,z) \quad (18)$$

where So is a source function and ρ_s is the scattered photon density, c is the velocity of light, D is the diffusion constant given by $D = 1/3\,[f_a+(1 - w)f_s]$, f_a and f_s are the absorption and scattering coefficient and related to K and S by

$$c\,K = f_a \quad (19)$$

$$c\,S = f_s \quad (20)$$

The solutions of Eq. 18 for both isotropic and an-isotropic scattering with various boundary conditions have been solved and successfully applied to design fiber optic oximeters in whole blood. The solution obtained by Reynolds for isotropically scattering homogeneous medium is [20]:

$$R\,(r_a) = (2/d)[S/(S+K)]\times \sum A_n\left[1 - e^{-d/\delta o}(-1)^n\right]\times [1-(2r/b)\,M_1N_1] \quad (21)$$

This equation gives diffuse reflectance for an illuminating optical fiber radius of b separated from the receiving fiber by r_a as a function of tissue thickness, d, and scattering and absorption constants, S and K. M1 and N1 are the first order Bessel functions. This equation can give quantitative diffuse reflectance from an isotropically scattering homogeneous medium such as whole blood.

In application to tissue, one-dimensional solution was applied to reflectance oximetry in blood and tissue by Longini, Cohen, et al. [53-54]. A three-dimensional solution for a two-layer tissue model was obtained by Takatani and Graham for application to reflectance oximetry from gut mucosa [55]. This solution was further extended by Schmitt to a multi-layer model application in pulse oximetry [56].

b. Time resolved case

When a narrow width light pulse, on the order of picoseconds, is injected into the medium, the transmitted pulse's shape and amplitude indicate the scattering and absorbing characteristics of the medium. The diffusion equation for a narrow width pulse through the medium can be written as [57]:

$$[(1/Dc)(\delta / \delta t) - (\Delta^2 - f_a / D)]\rho_s(r,\theta,z,t) = S'(r,\theta,z,t) \quad (22)$$

where, scattered photon density, $\rho_s(r, \theta, z, t)$, is now expressed as a time varying function. The local diffuse reflectance, R (r,t), from a semi-infinite medium irradiated by a pencil beam is given by [57];

Authorized licensed use limited to: Kansas State University. Downloaded on October 09,2021 at 04:47:57 UTC from IEEE Xplore. Restrictions apply.

APL_MAS_ITC_00374042
RX-0498.0005

$$R(r,t) = (4\pi Dc)^{-3/2} f_s^{-1} t^{-5/2} e^{-r/4DCt} e^{-f_a ct} \quad (23)$$

In the limit when time approaches infinity, the terminal slope of the $(\delta/\delta t)\log_e R(r, t)$ converges to;

$$\lim_{t \to \infty} (\delta / \delta t)\log_e R(r,t) = -f_a c \quad (24)$$

Thus, from Eq. 24, the absorption properties of the medium can be quantified.

In the frequency domain, the amplitude modulation and phase shift can be directly obtained from the Fourier transform of Eq. 22, with $S'(r, t) = N_0 \sin(\omega + \phi_0)$. Figure 6 shows a one-to-one transformation between the time resolved and frequency domain analyses. At low modulation frequency with $\omega << f_a c$ and $N = 1$, the mean of the distribution of pathlengths, $< L >$, is directly proportional to phase shift, ϕ (r, ω) which is given by [57];

$$\phi(r,\omega) = (3^{1/2} r\omega/2\pi c)[(1-w) f_s / f_a]^{1/2} \quad (25)$$

Since $\Delta\phi = \omega\Delta<L>/c$, then $<L>$ becomes:

$$\begin{aligned} < L > &= \Delta\phi c / \omega \\ &= (3^{1/2} r) / 2\pi[(1-w) f_s / f_a]^{1/2} \\ &= [3(1-w) f_s / f_a]^{1/2} r / 2\pi \quad (26) \end{aligned}$$

Since the scattering constant does not vary significantly with small wavelength changes, the ratio of the $<L>^2$ at two wavelengths will become the ratio of the absorption constants, thus giving hemoglobin saturation. Likewise, the phase shift information can also be used to obtain absorption characteristics of tissue that is dependent on hemoglobin oxygen saturation.

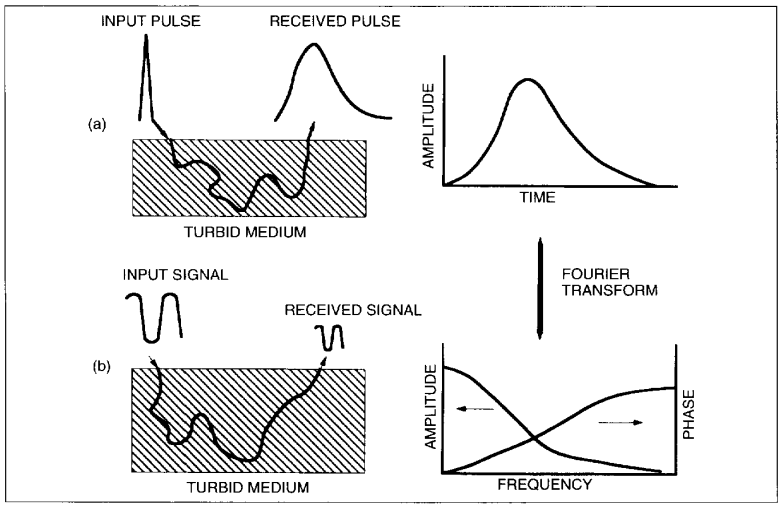

6. (a) Time and (b) frequency domain analysis of picosecond and ultra high frequency spectroscopy.

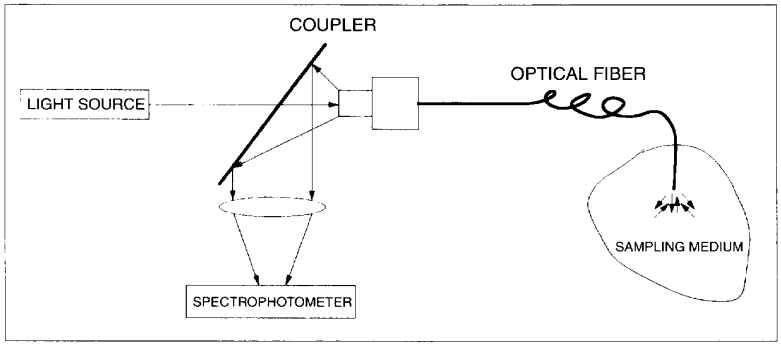

7. Basic block diagram of fiber-optic oximeter.

Invasive and Noninvasive Oximeter Systems

a) Intra- and extra-vascular oximetry

For intra-vascular oximetry, optical fibers are used to guide the light signal inside the vessel and reflected light from red blood cells back to the light detector (Fig. 7). In estimating SO_2, usually the reflectances at the two wavelengths, one in the red and the other in the near-infrared regions, are used with the empirical relation given below:

$$SO_2 = A + B(R\lambda_1 / R\lambda_2) \quad (27)$$

where A and B are the constants that depend on the fiber geometry and physiological parameters of blood. Equation 27 is the basis of modern reflection oximetry, derived empirically by Polany and Hehir [18]. Although the computation of reflectance ratios at wavelengths in the vicinity was suggested to cancel the effects of nonlinearity due to scattering, effects of hematocrit change may become important. Hence, currently available fiber-optic oximeters utilize more than two wavelengths to adjust for hematocrit variation. The fiber-optic oximeter from Oximetric (Oxnard, CA) utilizes three wavelengths to compensate for hematocrit changes.

Current use of intravascular oximeters is aimed at measurement of mixed venous saturation, from which status of circulatory system can be deduced. Mixed venous saturation varies in reflecting the changes of 1) SaO_2, 2) cardiac output, 3) hematocrit or hemoglobin content, and 4) oxygen consumption [6, 58-59]. One of the disadvantages of fiber optic oximeters is that damage to optical fibers results in severe measurement error. In order to circumvent this short-coming, catheter tip type oximeters using hybrid type miniature sensors have also been developed [60-61] (Figure 8).

In extra-vascular oximetry, forward scattered light through small vessels of frozen tissue samples, the messentery have also been analyzed to obtain oxygen saturation [62-64]. Multiple scattering theory (Eq. 18) has been utilized to treat scattering as an additive component to absorption. The oximeter sensor has also been applied to the extra-corporeal circuit used in the heart-lung machine to determine the oxygen saturation of the flowing blood [65-66].

b) Tissue oximetry

Tissue is a complicated medium in which blood vessels, both artery and vein, are distributed non-homogeneously. Red blood cells in arterial blood that flows

Authorized licensed use limited to: Kansas State University. Downloaded on October 09,2021 at 04:47:57 UTC from IEEE Xplore. Restrictions apply.

APL_MAS_ITC_00374043
RX-0498.0006

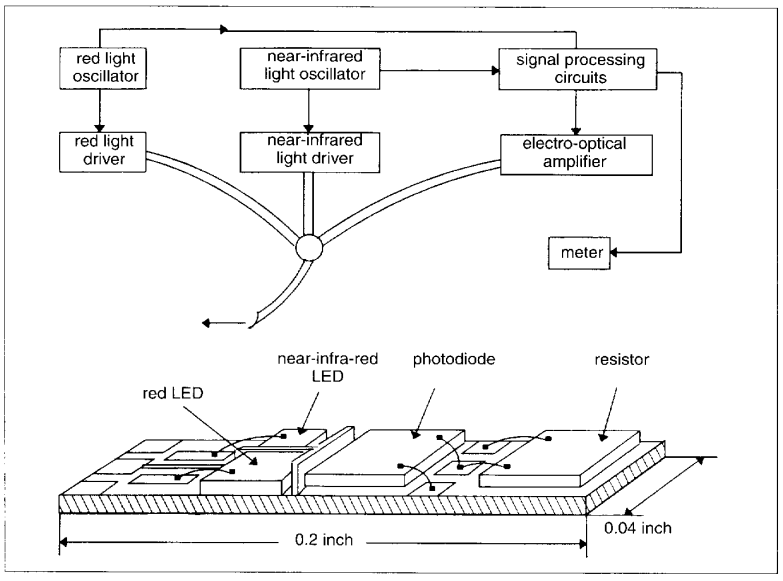

8. Basic illustration of the catheter-tip hybrid circuit oximeter sensor.

through the tissue release oxygen and return via the veinous system to the heart. Because of the unknown and nonhomogeneous distribution of arteries and veins, analysis of optical process in tissue is complex. Ever since the first tissue oximeter by Millikan, researchers have been trying to measure tissue oxygen saturation either in the transmission or reflection mode. The ear oximeter by Hewlett Packard Corp. has acquired some clinical success [67]. However, this instrument was never fully accepted. Arterialization of capillary blood by heating in the sensor created discomfort for patients. More importantly, the oximeter failed in the case of shock or hypo-volemia. The skin reflectance oximeter developed by Cohen [22] utilized solid state devices such as LEDs and photo-transistors. However, again because of a lack of calibration procedure, it did not attain clinical acceptance. Takatani [23,41,55], in 1979, developed a noninvasive tissue reflectance oximeter based on the photon diffusion theory and succeeded in estimation of mucosal oxygen saturation. Because of capillaries high density, the assumption to treat the tissue as a homogeneous mixture of blood and blood-free components was valid. The tissue was cooled to minimize arterial-to-venous saturation difference and tissue blood volume was measured by replacing the blood with saline. The arterial-to-venous saturation difference was minimized to less than 5% by cooling the tissue. The three-dimensional photon diffusion theory was used to compute the reflectances in the visible and near-infrared regions, which were then compared to the sampled tissue reflectances at five wavelengths. The theoretical predicted tissue saturation compared well with the average of the arterial and venous saturations. Approximately 70% of the blood was in the venous system of the gut mucosa.

1) Pulse oximetry

Pulse oximetry utilizes the plethysmographic principle in combination with the optical absorption characteristics of hemoglobin. The signal varies with pulsatile changes in tissue blood volume. The optical signal is usually sampled at two wavelengths and conventional linear regression analysis is applied to obtain arterial saturation. Pulse oximetry thus assumes that the pulsatile signal change is due to arterial blood volume change (Fig. 9). Most pulse oximeters are transmission type, where forward scattered light through the finger tip or the ear lobe is analyzed based on the Beer-Lambert law. An accuracy of 1% or better has been reported for the saturation range above 80%. Usually, the accuracy is less at lower saturation because of non-linear effects of absorption. Reflection type pulse oximeters have also been developed, with more general applicability to any portion of the body, such as forehead, cheek, calf and thigh (Fig. 10) [68-71]. However, in comparison to transmission, the reflection pulse oximeter has poorer signal-to-noise ratio. Mendelson, et al. utilized multiple photodiodes around the light source to enhance signal level, and a heater was incorporated in the sensor to warm the tissue so as to increase local blood flow [72-73]. Excellent correlation in comparison with the transmission oximeter has been shown from the calf and thigh. Takatani, et al. have studied the effect of light source and detector separation, and concluded that the greater the separation, the better the pulsatile to average signal level in the reflectance mode [74]. However, the absolute signal level decreased exponentially as the separation increased, and also the variability from person to person increased due to effects of tissue non-homogeneity. More light sources or light detectors are required to increase the signal level as well as to minimize the effects of tissue non-homogeneity.

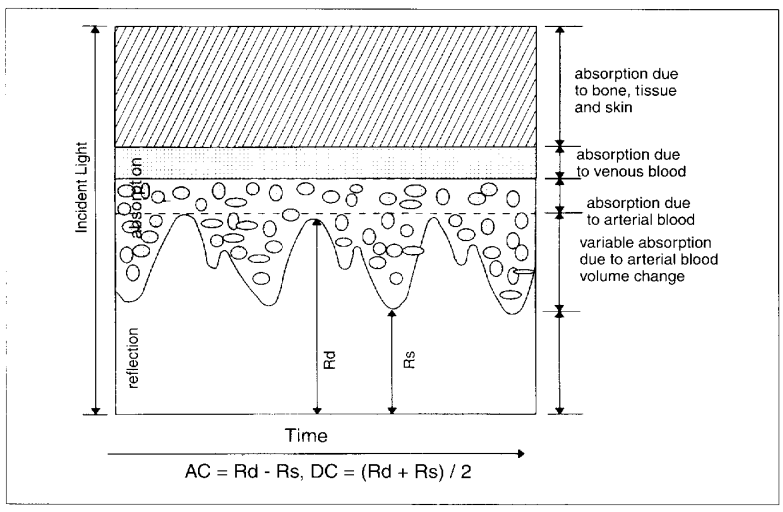

9. Conceptual tissue model for pulse oximetry.

Authorized licensed use limited to: Kansas State University. Downloaded on October 09,2021 at 04:47:57 UTC from IEEE Xplore. Restrictions apply.

APL_MAS_ITC_00374044
RX-0498.0007

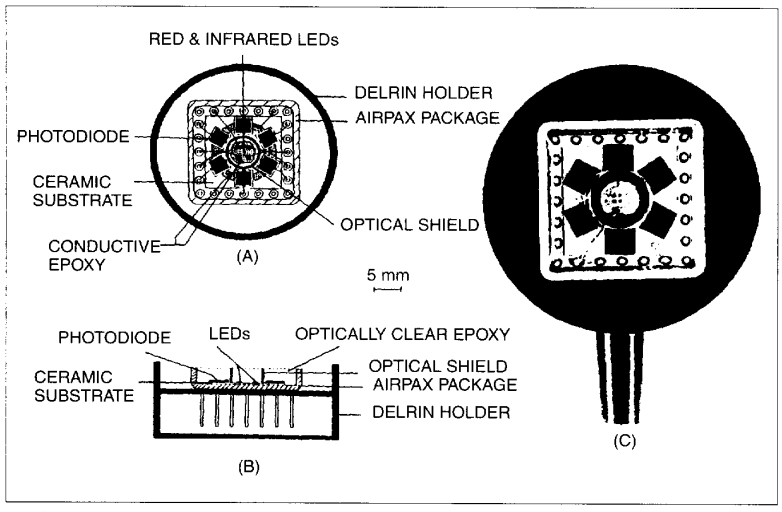

10. Schematic diagram of the reflectance oximeter sensor [68].

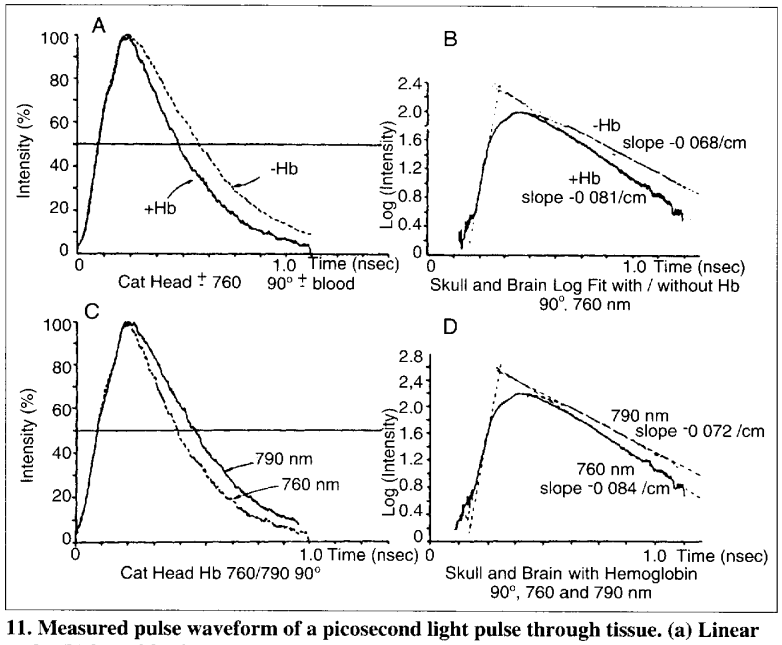

11. Measured pulse waveform of a picosecond light pulse through tissue. (a) Linear scale, (b) logarithmic scale, (c) effect of an alteration of wavelength from 790 to 760 nm in the cat-head model, a point at which the Hb absorbs maximially in this region [33], (d) logarithmic scale.

2) Time resolved spectroscopy

The major problem in analysis of tissue spectroscopy is the unknown pathlength, which precludes application of a simple Beer-Lambert law. When the optical pathlength is determined, optical density measurements based on the Beer-Lambert law allows computation of absorption in the tissue, assuming that the extinction due to scattering is minimal. In order to qunatitate this value, Chance, et al. and later Delpy, et al. applied a very narrow duration (picosecond order) pulse at the near-infrared region, where absorption due to hemoglobin and tissue is low, and measured the transit time of a photon through the tissue [31-35, 75-77]. Figure 11 shows the pulse wave after passing through the tissue. One can estimate the transit time as well as tissue scattering and absorption properties from this wave form. Similarly, frequency modulation, at frequencies on the order of 500 MHz, has been used to measure the phase shift through the tissue, from which transit time is calculated. According to the measurement performed by Delpy, et al., path length through an infant's head and arm is about 4 to 5 times larger than the separation distance of the light source and detector [78].

Time resolved spectroscopy is being applied to the area of neonatal cerebral monitoring [79-82]. A light signal is injected from one side of the head and scattered light through the head is measured at the opposite side. Figure 12 shows the instrumentation system to accomplish such measurement. The Beer-Lambert law is applied to analyze the measured signal in terms of oxy- and deoxy- hemoglobin concentrations. However, this method still lacks calibration. Thus, the result is still qualitative and only change with respect to the initial measurement can be followed. Also, the distribution of arterial and venous blood in the tissue is unknown. If the venous blood volume in tissue is assumed to be about 70-75%, venous saturation can be derived. Once these unknown areas are clarified, a very powerful technique will be available to map the oxygen field deep in the body, without invasive procedures.

In applications to the brain, McCormick, et al. [83] employed dual detectors as proposed also by Takatani, et al. [84]; one placed close to the light source and the other at a distance. Through differential measurement from these detectors, the effect of the skull was minimized and deep layer brain tissue information was obtained. Figure 13 shows how this concept works to eliminate surface or shallow layer effects. In the continous mode, the difference between the receivers one and two can be expressed using Eq. 13 as follows:

$$OD(\#1) = \alpha(bone)\, C(bone)\, d(bone) \tag{28}$$

$$OD(\#2) = \alpha(bone)\, C(bone)\, d(bone) + \alpha(brain)\, C(brain)\, d(brain) \tag{29}$$

$$OD(\#1) - OD(\#2) = \alpha(brain)\, C(brain)\, d(brain) \tag{30}$$

where α(bone) and α(brain) are the absorption coefficients; C(bone) and C(brain) are concentrations; and d(bone), d(brain) are the photon travel distances. Differential measurement allows detection of hemochrome concentration in a

Authorized licensed use limited to: Kansas State University. Downloaded on October 09,2021 at 04:47:57 UTC from IEEE Xplore. Restrictions apply.

APL_MAS_ITC_00374045
RX-0498.0008

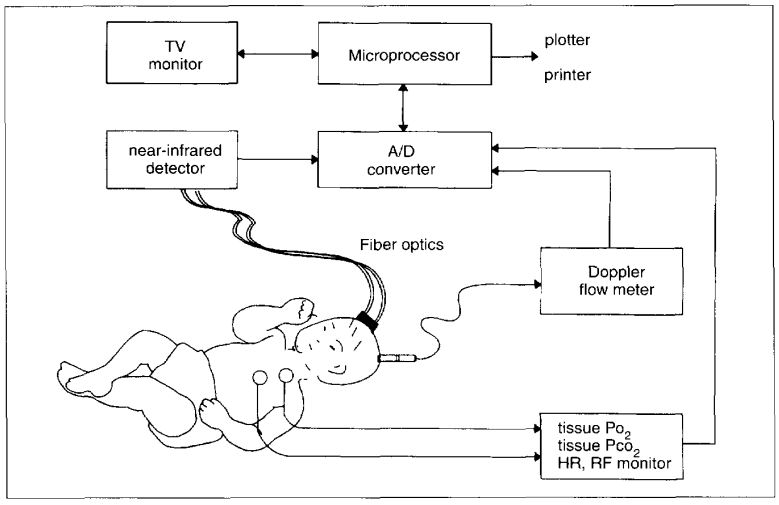

12. Block diagram of the neonatal cerebral monitoring system.

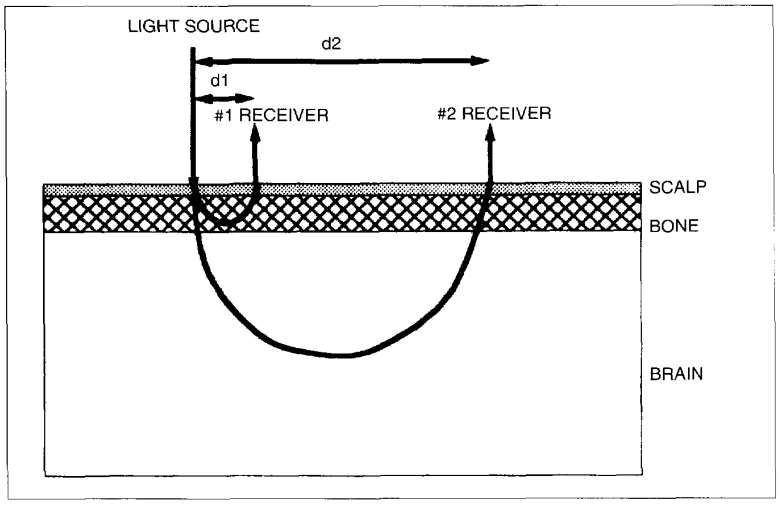

13. Near and far detector approach in estimation of deep layer tissue oxygenation as applied to the head.

deeper layer. Similar analysis is also applicable with time resolved spectroscopy. Transit time difference between detectors #1 and #2 can be obtained from Eqs. 23-24. In general, multiple detectors can be placed to focus at specific depths in tissue, yielding three-dimensional mapping of the oxygen field of tissue using time resolved diffusion equations.

Pulse spectroscopy is also applicable for the measurement of cytochrome aa3 saturation in the brain [38-39]. Although the concentration of cytochrome aa3 is considerably less than hemoglobin, photon counting techniques may yield information related to oxygenation of cytochrome at the mitochondria level. In combination with hemoglobin measurement, cytochrome and myoglobin measurements in tissue using time resolved oximetry will elucidate the mechanism of cell metabolism otherwise unattainable.

Summary

During the last decade, we have experienced two innovative approaches in spectroscopy. The first is pulse oximetry, which revolutionalized the clinical instrumentation. Because of limitations in application sites of the transmission oximeter, research continues on reflection oximeters. In the area of tissue oxygen monitoring, time resolved spectroscopy is gaining the interest of researchers. Picosecond pulse transit time measurements allow characterization of the tissue, from which oxygen saturation can be derived. However, we still lack adequate calibration procedure to quantitate optical measurements through the tissue. We need to build a good tissue model in which we can simulate real tissue with known arterial and venous distribution and oxygen saturation. Theoretical predictions can be compared to measured values in order to verify the applicability of tissue models. In addition to these measurements, imaging of tissue in terms of an oxygen field is becoming realistic. A three-dimensional oxygen field can be obtained through optical measurement, but first we need to quantitate accurately tissue arterial and venous blood volumes and oxygen saturations. Such a breakthrough will bring non-invasive optical spectroscopy into wide use in the diagnosis of circulatory disorders, the evaluation of the cardio-pulmonary system, and to determine the viability of various end-organs.

Setsuo Takatani obtained his B.S. with Distinction and M.S. in Electrical Engineering from the University of Oklahoma in 1971 and from Catholic University of America in 1974, respectively. He earned his Ph.D. in Biomedical Engineering from Case Western in 1978. He was a Fellow and Staff member of the Cleveland Clinic Foundation from 1979 through 1982. From 1982 to 1988, he was a Head of the Biomedical Instrumentation Lab, national Cardiovascular Center, Osaka, Japan. Since 1989, he has been Associate Professor, Department of Surgery, at the Baylor College of Medicine. In 1994, he also obtained the Doctor of Medicine Degree from Tokyo Medical and Dental University. His research interests include biomedical sensors and instrumentation, physiological system analysis, and artificial organs. He is a member of numerous medical societies including IEEE, BME, ASAIO, ISAO, ISOTT, and the Japanese societies of Artificial Organs and Medical Electronics.

Jian Ling received his B.S. degree from East China Normal University in 1986 and the M.S. degree from the University of Houston, both in electrical engineering. His master's research involved EEG signal

Authorized licensed use limited to: Kansas State University. Downloaded on October 09,2021 at 04:47:57 UTC from IEEE Xplore. Restrictions apply.

APL_MAS_ITC_00374046
RX-0498.0009

processing and pattern recognition. He is currently employed as a Research Assistant in the Department of Surgery, Baylor College of Medicine. He is involved in biomedical sensor projects including reflectance pulse oximetry and non-invasive blookd pressor monitoring, as well as the artificial heart project. His research interests include biomedical signal processing, neural networks, and medical instrumentation.

The authors may be reached at the Department of Surgery, Baylor College of Medicine, Houston, TX 77030.

References

1. **Antman EM, March JD, Green LH and Grossman W:** Blood oxygen measurements in the assessment of intracardiac left to right shunts: A critical appraisal of methodlogy. *Am J Cardiol* 46:265-271, 1980.

2. **Hillis LD, Firth BG, Winniford MD:** Variability of right-sided cardiac oxygen saturations in adults with and without left-to-right intracardiac shunting. *Am J Cardiol* 58:129-132, 1986.

3. **Davies GG, Jebson RJ, Glasgow BM and Hess DR:** Continuous Fick cardiac output compared to thermodilution cardiac output. *Critical Care Medicine* 14(10):881-885, 1986.

4. **Maekenzie GJ, Taylor SH, Flenley DC, and McDonald AH:** Circulatory and respiratory studies in myocardial infarction and cardiogenic shock. *Lancet* 2:825-832, 1964.

5. **Scheinman NM, Brown MA and Papaport E:** Critical assessment of use of central venous oxygen saturation as a mirror of mixed venous oxygen in severely ill cardiac patients. *Circulation* 40:165-172, 1969.

6. **Orland R:** Continuous mixed venous oximetry in critically ill surgical patients. *Arch Surg* 121:470-471, 1986.

7. **Valancia MD, and Burgess JH:** Arterial hypoxemia following acute myocardial infarction. *Circulation* 40:641-651, 1969.

8. **Severinghaus JW and Naifeh KH:** Accuracy of response of six pulse oximeters to profound hypoxia. *Anesthesiology* 67:551-558, 1987.

9. **Ryan CA, Barrington KJ, Vaughan D and Finer NN:** Directly measured arterial oxygen saturation in the newborn infant. *The Journal of Pediatrics* 109(3):526-529, 1986.

10. **Harris AP, Sendak MJ, Donham RT:** Changes in arterial oxygen saturation immediately after birth in the human neonate. *The Journal of Pediatrics* 109(1):117-119, 1986.

11. **Johnson N, Johnson V, Bannister J and Lilford RJ:** The accuracy of fetal pulse oximetry in the second stage of labor. *Neonatal Intensive Care* May/June 46-49, 1992.

12. **Brazy JE:** Cerebral oxygen monitoring with near infrared spectroscopy: Clinical application to neonates. *J Clin Monit* 7:325-334, 1991.

13. **Millikan, G.A:** The oximeter, an instrument for measuring continuously the oxygen saturation of arterial blood in man. *Rev of Scientific Instrument*, 13:434-444, 1942.

14. **Wood, EH, and Geraci, JE:** Photoelectric determination of arterial oxygen saturation in man. *J. Lab Clin Med.* 34:387-401, 1949.

15. **Brinkman, R and Sijlstra, WG:** Determination and continuous registration of the percentage oxygen saturation in clinical conditions. *Arch Chir Neerl* 1:177-183, 1949.

16. **Sekelj, P, Johnson, AL, Hoff, HE and Scherch, PM:** A photoelectric method for the determination of arterial oxygen saturation in man. *Amer Heart J.* 42:826-848, 1951.

17. **Tait, GR and Sekelj, P:** Analog computer for ear oximeter. *Med and Biol Engr* 5:463-472, 1967.

18. **Polanyi, ML and Hehir, RM:** New reflection oximeter. *Rev Sci Instru* 31(4):401-403, 1960.

19. **Cheung, PW:** Effects of blood physiological variations on optical scattering and fiberoptic oximetry. PhD. Dissertation, University of Washington, Seattle, WA 1973.

20. **Reynolds, LO:** Optical diffuse reflectance and transmittance from an anisotropically scattering finite blood medium. PhD Dissertation, University of Washington, Seattle, WA 1975.

21. **Johnson, CC:** Optical diffusion in blood. *IEEE Trans Biomed Engr.* BME-17(2):129-133, 1970.

22. **Cohen A and Wadsworth NA:** Light emitting diode skin reflectance oximeter. *Med Biol Eng* 10:385-391, 1972.

23. **Takatani, S, Cheung, PW and Ernst, EA:** Noninvasive tissue reflectance oximeter: An instrument for tissue hemoglobin oxygen saturation in vivo. *Annals of Biomed Engr* 8:1-15, 1980.

24. **Wodick, R and Lubbers, DW:** Quantitative evaluation of reflection spectra of living tissues. Hoppe-Seyler's *Z. Physiol Chem* 355:583-594, 1974.

25. **Lubbers, WD and Wodick R:** The examination of multicomponent systems in biological materials by means of a rapid scanning photometer. *Applied Optics* 8(5):1055-1062, 1969.

26. **Aoyagi, T, Kishi, M, Yamaguchi, K:** Improvement of the ear-piece oximeter. 13th Annual Meeting of Japanese Soc med Electronics and Biomed Eng. 90-91, 1974.

27. **Yelderman, M and New W:** Evaluation of pulse oximetry. *Anesthesiology* 59:349-352, 1983.

28. **Pologe, JA:** Pulse oximetry; technical aspects of machine design. *Int Anesthesiology Clin* 25:137-153, 1987.

29. **Kellerman AL, Cofer CA, Joseph S, Backman BB:** Impact of portable pulse oximetry on arterial blood gas test ordering in an urban emergency department. *Annals of Emergency Medicine* 20(2):130-134, 1991.

30. **Szaflarski NL and Cohen NH:** Use of pulse oximetry in critically ill adults. *Heart and Lung* 18(5):444-455, 1989.

31. **Delpy DT, Cope M, van der Zee P, Arridge S, Wray S and Wyatt J:** Estimation of optical path length. *Phys Med Biol* 33:1433-1442, 1988.

32. **Jacques SL and Flock ST:** Time-resolved reflectance spectroscopy. *SPIE Proceedings* 1525:35-40, 1991.

33. **Chance B, Leigh H, Miyake H, Smith D, Nioka S, et al:** Comparison of time resolved and un-resolved measurements of deoxyhemoglobin in brain. *Proc Natil Acd Sci.* 85:4971-4975, 1988.

34. **Jacques SL:** Principles of phase-resolved optical measurements. *SPIE Proceedings* 1525:143-153, 1991.

35. **Chance B, Haselgrove J, Wang NG, Maris M and Sevick E:** Photon dynamics in tissue imaging. *SPIE* 1525:68-82, 1991.

36. **Singer JR, Grunbaum FA, Kohn P and Zubelli JP:** Image reconstruction of interior of bodies that diffusion radiation. *Science* 248:990-993, 1990.

37. **Jobsis FF, Keizer JH, LaManna JC, Rosenthal M:** Reflection spectrophotometry of cytochrome aa3 in vivo. *J Appl Physiol*: Respirat. Environ. exercise Physiol. 43(5):858-872, 1977.

38. **Kariman K, Jobsis FF and Saltzman H:** Cytochrome aa3 reoxidation: Early indicator of metabolic recovery from hemorrhagic shock in rats. *J Clin Invest* 72:180-191,1983.

39. **Van Assendelft OW:** *Spectrophotometry of hemoglobin derivatives.* Assen, The Netherlands, Royal Vangorcum Ltd. 1970.

40. **Wilson BW:** Optical properties of tissues. *Encyclopedia of Human Biology* 5:587-597, 1991.

41. **Takatani S:** On the theory and development of a non-invasive tissue reflectance oximeter. PhD Dissertation, Case Western Reserve University, Cleveland, OH, 1978.

42. **Bruls WAG and van der Leun JC:** Forward scattering properties of human epidermial layers. *Photochem and photobiol* 40:231-242, 1984.

43. **van Gemert MJC, Henning JPH:** A model approach to laser coagulation of dermal vascular lesions. *Arch Dermatol Res* 270:429-439, 1981.

44. **Wilson BC, Patterson MS and Burns DM:** Effect of photosensitizer concentration in tissue on the penetration depth of phtoactivating light. *Lasers Med Sci* 1:235-244, 1986.

45. **Flock ST, Wilson BC, Patterson MS:** Total attenuation coefficients and scattering function of tissues and phantom materials at 633 nm. *Med Phys* 14:835-841, 1987.

46. **Marynissen JPA and Star WM:** Phantom measurements for light dosimetry using isotropic and small aperture detectors. In Porphyrin Localization and Treatment of Tumors, Doiron DR and Gomen, eds. Liss, New York, 1984. pp 133-138.

47. **Lin JC and Guy AW:** A note on the optical scattering characteristics of whole blood. *IEEE Trans Biomed Engr.* 43-45, 1974.

48. **Ross DA:** Scattering by finite volume dielectric objects. PhD Dissertation, University of Washington, Seattle, WA, 1969.

49. **Twersky V:** Absorption and multiple scattering by biological suspensions. *J Opt Soc Amer* 60:1084-1093, 1970.

50. **Schuster A:** Radiation through a foggy atmosphere. *Astrophys J* 21:1-22, 1905.

51. **Kubelka P and Munk F:** Ein Beitrang zur Optik der Farbanstriche. *Z techn Phys* 12:593-601, 1931.

52. **Ishimaru A:** *Wave Propagation and Scattering in Random Media.* Academic Press, New York, 1978.

53. **Longini RL and Zdrojkowski R:** A note on the theory of backscattering of light by living tissue. *IEEE Trans Biomed Engr.* BME-15(1):4-10, 1968.

54. **Cohen A and Longini RL:** Theoretical deter-

Authorized licensed use limited to: Kansas State University. Downloaded on October 09,2021 at 04:47:57 UTC from IEEE Xplore. Restrictions apply.

APL_MAS_ITC_00374047
RX-0498.0010

mination of the blood relative oxygen saturation in vivo. *Med and Biol Eng* 9:61-69, 1971.

55. **Takatani S and Graham MD:** Theoretical analysis of diffuse reflectance from a two-layer tissue model. *IEEE Trans Biomed Engr.* BME-26(12):656-664, 1979.

56. **Schmitt JM, Zhou GX, Walker EC and Wall RT:** Multilayer model of photon diffusion in skin. *J Opt Soc Am* 7(11):2141-2153, 1990.

57. **Wilson BC, Sevick EM, Patterson MS, Chance B:** Time-dependent optical spectroscopy and imaging for biomedical applications. *Proceedings of the IEEE* 80(6):918-930, 1992.

58. **Nelson LD:** Continuous venous oximetry in surgical patients. *Ann Surg* 203(3):329-333, 1986.

59. **Takatani S:** Open loop analysis of circulatory system in awake live animals: Relation between mixed venous saturation and hemodynamic and metabolic variables. Artificial Organs 17(2):79-91, 1993.

60. **Yee S, Schibli E and Krishnan V:** A proposed miniature red/infrared oximeter suitable for mounting on a catheter tip. *IEEE Trans Biomed Eng* BME-24(2):195-197, 1977.

61. **Schmitt JM, Meindl JD, Mihm RG:** An integrated circuit-based optical sensor for in vivo measurement of blood oxygenation. *IEEE Trans Biomed Eng* BME-33(2):98-107, 1986.

62. **Pittman RN and Duling BR:** Measurement of percent oxyhemoglobin in the microvasculature. *J Appl Phsiol.* 38(2):321-327, 1975.

63. **Pittman RN and Duling BR:** A new method for the measurement of percent oxygehemoglobin. *J Appl Physiol* 38(2):315-320, 1975.

64. **Sinha AK, Neubauer JA, Lipp JA and Weiss HR:** Blood oxygen saturation determination in frozen tissue. *Micrvascular Research* 14:133-144, 1977.

65. **Vurek GG, Kolobow T, Pegram SE, and Friauf WS:** Oxygen saturation monitor for extracorporeal circulation applications. *Med Instru* 7(4):262-267, 1973.

66. **Takatani S, Noda H, Takano H and Akutsu T:** A miniature hybrid reflection type optical sensor for measurement of hemoglobin content and oxygen saturation of whole blood. *IEEE Trans Biomed Eng* 35:187-198, 1988.

67. **Merrick EB, Bayes TJ:** Continuous, nonivasive measurements of arterial blood oxygen levels. *Hewlett-Packard J* 28:2-9, 1976.

68. **Mendelson Y, Kent JC, Yocum BL, and Birle M:** Design and evaluation of a new reflectance pulse oximeter sensor. *Medical Instrumentation* 22(4):167-173, 1988.

69. **Shimada Y, Nakashima K, Fujiwara Y, Komatsu T, Kawanishi M, et al.,** Evaluation of a new reflectance pulse oximeter for clinical applicability. *Med Biol Eng.* 29:557-561, 1991.

70. **Decker MJ, Dickensheets D, Arnold JL, Cheung PW and Strohl KP:** A comparison of a new reflectance oximeter with the Hewlett-Packard ear oximeter. 24:122-126, 1990.

71. **Takatani S, Davies C, Sakakibara N, Zurick A, Kraenzler E, Golding L, Noon GP, Nose Y and DeBakey ME:** Experimental and clinical evaluation of a noninvasive reflectance pulse oximeter sensor. *J Clin Monit* 8:257-266, 1992.

72. **Mendelson Y and Yocum B:** Noninvasive measurement of arterial oxyhemoglobin saturation with a heated and a non-heated skin reflectance pulse oximeter sensor. *Biomedical Instrumentation and Technology* 25:472-480, 1991.

73. **Mendelson Y and McGinn MJ:** Skin reflectance pulse oximetry: In vivo measurements from the forearm and calf. *J Clin Monit* 7:7-12, 1991.

74. **Ling J, Takatani S, Noon GP and Nose Y:** In vivo studies of reflectance pulse oximeter sensor. *SPIE Proceedings*, 1993 (in press).

75. **Chance B, Wang NG, Maris M, Nioka S and Sevik E:** Quantitation of tissue optical characteristics and hemoglobin desaturation by time and frequency resolved multi-wavelength spectrophotometry. *Oxygen Transport to Tissue* 14:297-304, 1992.

76. **Nomura Y and Tamura M:** Picosecond time of flight measurement of living tissue: Time resolved Beer-Lambert Law. *Oxygen Transport to Tissue* 14: 131-136, 1992.

77. **Kessler FK, Wiesner J and Wokaun A:** Analysis of multiple multipole scattering by time-resolved spectroscopy and angular dependent spectrometry. *Oxygen Transport to Tissue* 14: 261-266, 1992.

78. **van der Zee P, Cope M, Arridge SR, Essenpreis M, Potter LA, et al:** Experimentally measured optical pathlengths for the adult head, calf and forearm and the head of the newborn infant as a function of inter optode spacing. *Oxygen Trasnport to Tissue* 14: 143-153, 1992.

79. **Brazy JE:** Cerebral oxygen monitoring with near infrared spectroscopy. Clinical application to neonates. *J Clin Monit* 7:325-334, 1991.

80. **Hazeki O, Tamura M:** Quantitative analysis of hemoglobin oxygenation state of rat brain in situ by near-infrared spectrophotometry. *J Appl Physiol* 64:796-802, 1988.

81. **Elwell CE, Cope M, Edwards AD, Wyatt JS, Reynolds EOR et al:** Meausrement of cerebral blood flow in adult humans using near infrared spectroscopy - Methodology and possible errors. *Oxygen Transport to Tissue* 14:235-245, 1992.

82. **Kurth CD, Steven JM, Benaron D and Chance B:** Near-infrared monitoring of the cerebral circulation. *J Clin Monit* 9:163-170, 1993.

83. **McCormick PW, Stewart M, Goetting MG, Dujovny M, Lewis G et al:** Noninvasive cerebral optical spectroscopy for monitoring cerebral oxygen delivery and hemodynamics. *Critical Care Medicine* 19(1):89-97, 1991.

84. **Takatani S, Awazu K, Kanda M and Takano H:** Theoretical consideration for design of optical sensor for nonivnasive tissue reflectance oximetry. *Proceedings of Jap Soc of ME & BE* 26:222, 1988.

Authorized licensed use limited to: Kansas State University. Downloaded on October 09,2021 at 04:47:57 UTC from IEEE Xplore. Restrictions apply.

APL_MAS_ITC_00374048
RX-0498.0011